EXPERIMENT DESIGN WITH CONTROL GUARANTEES

DANIEL Y ENRIQUE

Abstract. We study deterministic experiment design for continuous-time linear time-invariant systems with the goal of certifying controllability properties directly from data. We show that structured input families can generically reveal the controllability rank from finitely many state snapshots (or terminal states): polynomial, exponential, and sinusoidal excitations are persistently exciting, and a single suitably parameterized trajectory suffices to recover the controllable subspace almost everywhere. Complementarily, we develop a continuous-time, data-driven analogue of the Hautus (PBH) test based on residual Gramians and a derivative-free cross-moment formulation, and we provide basic high-probability error bounds under an Itô noise model. Finally, we derive sharp input designs that optimally condition the relevant Gramians under L^2 energy and H^1 smoothness budgets.

Contents

†Chair for Dynamics, Control, Machine Learning, and Numerics (Alexander von Humboldt Professorship), Department of Mathematics, Friedrich-Alexander-Universität Erlangen-Nürnberg, 91058 Erlangen, Germany.

2020 *Mathematics Subject Classification.* 35B40, 45K05, 74F05.

Key words and phrases. Experiment design, Controllability, Persistent excitation, Linear systems, System identification.

1. Introduction

Motivation: learning models that are *control-relevant*. Modern system identification and data-driven control rely on experiments that generate *informative* data, so that the learned model supports reliable closed-loop guarantees. In particular, for linear systems, a fundamental prerequisite for many synthesis and certification tasks is that the data reveals the system's *controllable subspace* and, ideally, certifies controllability. However, learning objectives that focus only on trajectory matching (prediction or simulation error) do *not* automatically preserve control-theoretic properties such as controllability or stabilizability, since distinct systems can generate similar trajectories on a finite horizon while having different reachable dynamics. This gap motivates experiment design criteria that directly encode control-relevant identifiability.

Persistent excitation and universality in data-driven control. The classical notion of *persistent excitation* formalizes the idea that the input must excite all relevant degrees of freedom so that system parameters (or behaviors) become identifiable [15]. In the behavioral framework, Willems' Fundamental Lemma states that, for controllable LTI systems, all finite-length trajectories can be parameterized from a single measured trajectory provided the input is persistently exciting of sufficiently high order [15]. This principle underpins a large class of methods for data-driven simulation and control and has been extended in several directions, including multiple datasets and rank-based characterizations [14, 12]. Recent developments also highlight a converse viewpoint: if one seeks a single experiment design that works *uniformly* for broad classes of controllable systems ("universal" inputs), then persistent excitation is not merely sufficient but essentially necessary at the right order [9]. For continuous-time systems, related identifiability conditions and continuous-time variants of Willems-type results have also been investigated [8, 7].

Offline vs. online experiment design. Most classical guidance concerns *offline* experiment design, where one selects a fixed open-loop excitation signal before collecting data. Offline designs are attractive because they are universal and simple to implement, but they can be conservative and sample-inefficient. This has motivated *online* (adaptive) experiment design methods that adjust the input in real time based on the observed data to accelerate identifiability and reduce the amount of data required [11, 3]. In fact, sharp sample-efficiency results have recently been obtained for the length of an informative trajectory needed for linear system identification [1]. These developments emphasize that experiment design should be treated as a first-class component of safe data-driven control, rather than a preprocessing step.

Controllability certification from data. Alongside trajectory-based learning, there is a growing literature on *control-theoretic tests from data*, including controllability/stabilizability certificates that avoid explicit system identification. In discrete time, informativity-based tests provide purely data-dependent rank conditions for control properties [12, 4]. More recently, Mishra et al. developed algebraic data-driven tests for controllability of LTI systems from batches of measurements [6]. These results collectively suggest that controllability can, in principle, be certified directly from suitably designed experiments, even when the system matrices are unknown.

Scope of this paper. In this work we revisit experiment design for LTI systems from the perspective of certifying the *dimension of the controllable subspace*. Let $(\mathbf{A}, \mathbf{B})$ be unknown and

consider the continuous-time LTI dynamics

$$\dot{x}(t) = \mathbf{A}x(t) + \mathbf{B}u(t), \qquad x(0) = 0.$$

The controllable subspace is characterized by the reachability matrix

$$\mathbf{C} := [\mathbf{B}, \mathbf{AB}, \ldots, \mathbf{A}^{n-1}\mathbf{B}],$$

and its rank $r := \operatorname{rank}(\mathbf{C})$ [5, 2]. Rather than assuming stochastic richness or averaging over random inputs, we study *structured deterministic* input families that are *persistently exciting in a generic sense*, meaning that for almost all parameters (and, in the snapshot setting, for generic distinct sampling times) they induce snapshot matrices whose rank equals r (Definition 2.1). This yields identifiability guarantees that are constructive and compatible with deterministic experiment design.

1.1. Main Contributions.

- **A continuous-time data-driven Hautus margin.** Complementing terminal-state guarantees, we provide a continuous-time, data-driven analogue of the classical Hautus (PBH) test [10], based on the residual Gramian $\mathbf{G}_\lambda(u) = \int_0^T (\dot{x}(t) - \lambda x(t))(\dot{x}(t) - \lambda x(t))^* \, \mathrm{d}t$ and its frequency-domain representation.

  $$(\mathbf{A}, \mathbf{B}) \text{ is controllable} \quad \Leftrightarrow \quad \operatorname{rank}(\mathbf{G}_\lambda(u)) = n \text{ for all } \lambda \in \mathbb{C}.$$

  We further develop a derivative-free cross-moment formulation and give basic concentration bounds under an Itô noise model

  $$\mathrm{d}x(t) = \Big(\mathbf{A}x(t) + \mathbf{B}u(t)\Big)\,\mathrm{d}t + \beta\,\mathrm{d}W(t).$$

- **Input design for conditioning the Hautus margin.** We provide sharp, model-agnostic designs for conditioning the input Gramian $\mathbf{S}_U(u) = \int_0^T u(t)u(t)^\top \, \mathrm{d}t$, which in turn stabilizes the data-driven Hautus margin. Under an L^2 energy budget, the best possible conditioning is achieved by choosing m orthonormal time functions (isotropic $\mathbf{S}_U(u)$; Proposition 3.8). Under an H^1 smoothness budget, the optimal isotropic design is given by the first m Neumann modes on $[0, T]$, i.e., the constant mode and cosines $\cos(k\pi t/T)$ (Proposition 3.10).

Together, these results provide a principled experiment-design toolkit for learning models that preserve controllability structure and are therefore suitable for safe downstream control.

2. Problem Statement

We consider the continuous-time Linear Time-Invariant (LTI) system

$$\dot{x}(t) = \mathbf{A}x(t) + \mathbf{B}u(t), \tag{1}$$

where the matrices $\mathbf{A} \in \mathbb{R}^{n\times n}$ and $\mathbf{B} \in \mathbb{R}^{n\times m}$ are unknown. The solution is

$$x(t) = e^{\mathbf{A}t}x(0) + \int_0^t e^{\mathbf{A}(t-\tau)}\mathbf{B}\,u(\tau)\,\mathrm{d}\tau.$$

For simplicity, we assume the initial state is zero, $x(0) = 0$. A fundamental property of the system is **controllability**, which characterizes the ability to steer the state throughout the full state space. The reachable (controllable) subspace from the origin is characterized by the controllability matrix

$$\mathbf{C} = [\mathbf{B},\ \mathbf{AB},\ \mathbf{A}^2\mathbf{B},\ \cdots,\ \mathbf{A}^{n-1}\mathbf{B}].$$

Let $r := \operatorname{rank}(\mathbf{C})$ denote the dimension of the controllable subspace [5, 2]; the pair $(\mathbf{A}, \mathbf{B})$ is controllable if and only if $r = n$. Our objective is to design inputs $u(t)$ such that observed

trajectories reveal r from finitely many snapshots. If only outputs $y(t) = \mathbf{C}_y x(t)$ are measured (with known $\mathbf{C}_y \in \mathbb{R}^{p\times n}$), then the same rank statements apply to the output-restricted reachability matrix $\mathbf{C}_y\mathbf{C}$.

The definition below formalizes a deterministic, generic notion of "informativeness" that is common to all of our proofs: (i) the trajectory stays in the controllable subspace, (ii) the chosen input family produces enough distinguishable time signatures to identify vector coefficients, and (iii) those coefficients generically span the controllable subspace.

Definition 2.1 (Persistently exciting inputs)**.** A parameterized family of inputs $\{u_\theta\}_{\theta\in\Theta}$ is *persistently exciting* if, for every pair $(\mathbf{A}, \mathbf{B})$ with controllability rank $r := \operatorname{rank}(\mathbf{C})$, there exist an integer $N \geq r$ and a horizon $T > 0$ such that, for Lebesgue almost every admissible parameter choice (a single θ in (i), or the tuple $(\theta_1, \ldots, \theta_N)$ in (ii)), the corresponding data matrix has rank exactly r. Concretely, the data matrix is taken to be either: (i) *single-trajectory snapshots* $[x_\theta(t_1), \ldots, x_\theta(t_N)]$ from one experiment, where $t_1, \ldots, t_N \in (0, T]$ are pairwise distinct sampling times fixed in advance; or (ii) *multi-trajectory terminal states* $[x_{\theta_1}(T), \ldots, x_{\theta_N}(T)]$ from N experiments at a common terminal time T (so repeated sampling times are allowed across experiments).

3. Data-Driven Hautus Tests for Continuous-Time Systems

One route to certifying controllability (more precisely, the dimension of the controllable subspace) from data is via terminal-state information under structural assumptions (e.g., a fixed initial condition and structured input families). Here we develop an alternative route based on rank conditions that are equivalent to controllability/stabilizability. For continuous-time LTI systems (1), the classical Hautus (PBH) test [10, Theorem 3.13] states:

- $(\mathbf{A}, \mathbf{B})$ is controllable if and only if $\operatorname{rank}\begin{bmatrix}\mathbf{A} - \lambda\mathbf{I} & \mathbf{B}\end{bmatrix} = n$ for all $\lambda \in \mathbb{C}$;
- $(\mathbf{A}, \mathbf{B})$ is stabilizable if and only if $\operatorname{rank}\begin{bmatrix}\mathbf{A} - \lambda\mathbf{I} & \mathbf{B}\end{bmatrix} = n$ for all $\lambda \in \mathbb{C}$ with $\Re(\lambda) \geq 0$.

Using only measured data, one can test controllability/stabilizability without explicitly identifying $(\mathbf{A}, \mathbf{B})$; see [12, 4] for the discrete-time case. Here we state a continuous-time version based on time-domain moments of the state and input signals.

Data model. We assume access to $u(\cdot)$ and the resulting state $x(\cdot)$ on a finite horizon $[0, T]$ (either as a continuous-time record or via sufficiently fine sampling so that the integrals below can be approximated numerically). When $\dot{x}$ is not directly available or is too noisy to estimate reliably, we rely on the cross-moment formulation in Section 3.2, which only uses increments of x in the stochastic setting and avoids forming $\dot{x}$ in the deterministic setting.

Outline. We first introduce a residual Gramian $\mathbf{G}_\lambda(u)$ whose invertibility for all $\lambda \in \mathbb{C}$ is equivalent to controllability under a mild data-richness condition. We then develop a derivative-free cross-moment formulation (deterministic and Itô) that enables estimating $\mathbf{G}_\lambda(u)$ and a corresponding Hautus margin directly from measured data. Finally, we give an operator formulation that reduces checking all $\lambda \in \mathbb{C}$ to a finite candidate set and discuss a simple L^2-budget design principle for conditioning the input Gramian.

3.1. Time-domain Gramian formulation.

For input design it is convenient to work with a continuous-time analogue in which rank is replaced by a coercive quadratic functional.

Fix a horizon $T > 0$ and let $u \in L^2(0, T; \mathbb{R}^m)$ be an input generating an absolutely continuous state trajectory $x : [0, T] \to \mathbb{R}^n$ with $x, \dot{x} \in L^2(0, T; \mathbb{R}^n)$. For $\lambda \in \mathbb{C}$ define the residual signal and its (time-domain) Gramian

$$m_\lambda(t) := \dot{x}(t) - \lambda x(t) \in \mathbb{C}^n, \qquad \mathbf{G}_\lambda(u) := \int_0^T m_\lambda(t) m_\lambda(t)^* \, \mathrm{d}t \in \mathbb{C}^{n\times n}.$$

Define the stacked signal and its Gramian

$$z(t) := \begin{bmatrix} x(t) \\ u(t) \end{bmatrix} \in \mathbb{R}^{n+m}, \qquad \mathbf{S}_Z(u) := \int_0^T z(t)z(t)^\top \, \mathrm{d}t \in \mathbb{R}^{(n+m)\times(n+m)}.$$

Finally, define the Hautus matrix

$$\mathbf{P}_\lambda := \begin{bmatrix} \mathbf{A} - \lambda \mathbf{I} & \mathbf{B} \end{bmatrix} \in \mathbb{C}^{n\times(n+m)}.$$

Note that $\mathbf{S}_Z(u) \succeq 0$ and $\mathbf{G}_\lambda(u) \succeq 0$ by construction. Moreover, for every admissible input u,

$$m_\lambda(t) = (\mathbf{A} - \lambda \mathbf{I})x(t) + \mathbf{B}u(t) = \mathbf{P}_\lambda z(t) \quad \text{for a.e. } t \in (0, T),$$

and therefore

$$\mathbf{G}_\lambda(u) = \mathbf{P}_\lambda \mathbf{S}_Z(u) \mathbf{P}_\lambda^*. \tag{2}$$

Frequency-domain representation. To relate this to a Fourier-domain statistic, view m_λ as a time-limited signal extended by zero outside $[0, T]$. That is, define $\tilde{m}_\lambda(t) := m_\lambda(t)\mathbb{1}_{[0,T]}(t)$ and its Fourier transform by

$$\widehat{m}_\lambda(\mathrm{i}\omega) := \int_{\mathbb{R}} \tilde{m}_\lambda(t) e^{-\mathrm{i}\omega t} \, \mathrm{d}t = \int_0^T m_\lambda(t) e^{-\mathrm{i}\omega t} \, \mathrm{d}t, \qquad \omega \in \mathbb{R}.$$

By the Plancherel theorem (Parseval identity) with this convention,

$$\mathbf{G}_\lambda(u) = \int_{\mathbb{R}} \widehat{m}_\lambda(\mathrm{i}\omega) \widehat{m}_\lambda(\mathrm{i}\omega)^* \, \frac{\mathrm{d}\omega}{2\pi}. \tag{3}$$

This yields a direct frequency-domain analogue of the time-domain margin $\sigma_{\min}(\mathbf{G}_\lambda(u))$. In practice, one evaluates $\sigma_{\min}(\mathbf{G}_\lambda(u))$ on a finite set of λ (e.g., a grid or the candidate values discussed below). Working with $\widehat{m}_\lambda$ directly avoids integration-by-parts boundary terms. Indeed, for $\widehat{x}(\mathrm{i}\omega) := \int_0^T x(t) e^{-\mathrm{i}\omega t} \, \mathrm{d}t$, integration by parts gives

$$\int_0^T \dot{x}(t) e^{-\mathrm{i}\omega t} \, \mathrm{d}t = x(T)e^{-\mathrm{i}\omega T} - x(0) + \mathrm{i}\omega \widehat{x}(\mathrm{i}\omega),$$

hence

$$\widehat{m}_\lambda(\mathrm{i}\omega) = (\mathrm{i}\omega - \lambda)\widehat{x}(\mathrm{i}\omega) + x(T)e^{-\mathrm{i}\omega T} - x(0).$$

Fix $v \in \mathbb{C}^n$. Since $\mathbf{P}_\lambda \mathbf{S}_Z(u) \mathbf{P}_\lambda^* \succeq 0$ and $\mathbf{S}_Z(u) \succeq 0$,

$$v^* \mathbf{P}_\lambda \mathbf{S}_Z(u) \mathbf{P}_\lambda^* v = (\mathbf{P}_\lambda^* v)^* \mathbf{S}_Z(u) (\mathbf{P}_\lambda^* v) \geq \sigma_{\min}(\mathbf{S}_Z(u)) \, \|\mathbf{P}_\lambda^* v\|_2^2.$$

By definition of $\sigma_{\min}$, $\|\mathbf{P}_\lambda^* v\|_2 \geq \sigma_{\min}(\mathbf{P}_\lambda^*)\|v\|_2 = \sigma_{\min}(\mathbf{P}_\lambda)\|v\|_2$. Taking the minimum over $\|v\|_2 = 1$ and using (2) yields

$$\sigma_{\min}\Big(\mathbf{G}_\lambda(u)\Big) = \sigma_{\min}(\mathbf{P}_\lambda \mathbf{S}_Z(u) \mathbf{P}_\lambda^*) \geq \sigma_{\min}(\mathbf{P}_\lambda)^2 \, \sigma_{\min}\Big(\mathbf{S}_Z(u)\Big).$$

This bound holds for every $\lambda \in \mathbb{C}$.

Theorem 3.1 (Continuous Hautus Test). *If there exists u such that $\operatorname{rank}(\mathbf{G}_\lambda(u)) = n$ for all $\lambda \in \mathbb{C}$, then $(\mathbf{A}, \mathbf{B})$ is controllable. Moreover, if $\mathbf{S}_Z(u)$ is invertible, then the converse holds*

$$(\mathbf{A}, \mathbf{B}) \text{ is controllable} \quad \Leftrightarrow \quad \operatorname{rank}(\mathbf{G}_\lambda(u)) = n \text{ for all } \lambda \in \mathbb{C}.$$

Proof. See Appendix A.1. □

3.2. **Stochastic model and Itô residual.** Another alternative to direct state-derivative measurements is to estimate $\mathbf{P}_\lambda$, and hence $\mathbf{G}_\lambda(u)$, from cross-moments between the state and input signals, using only increments of x. This is particularly natural in a stochastic setting, where $\dot{x}$ does not exist pointwise. Assume that the measured state is an Itô process satisfying the linear SDE

$$\mathrm{d}x(t) = \Big(\mathbf{A}x(t) + \mathbf{B}u(t)\Big)\,\mathrm{d}t + \beta\,\mathrm{d}W(t), \qquad t \in [0,T],$$

where W is a q-dimensional standard Brownian motion and $\beta \in \mathbb{R}^{n\times q}$ is constant. For $\lambda \in \mathbb{C}$, define the Itô residual differential

$$\mathrm{d}y_\lambda(t) := \mathrm{d}x(t) - \lambda x(t)\,\mathrm{d}t = \mathbf{P}_\lambda z(t)\,\mathrm{d}t + \beta\,\mathrm{d}W(t). \tag{4}$$

Cross-moment factorization. Define the (matrix-valued) cross-moment

$$\mathbf{H}_\lambda(T) := \int_0^T \mathrm{d}y_\lambda(t)\, z(t)^\top \in \mathbb{C}^{n\times(n+m)}, \tag{5}$$

and recall $\mathbf{S}_Z(u) = \int_0^T z(t)z(t)^\top\,\mathrm{d}t$. Plugging (4) into (5) yields the exact decomposition

$$\mathbf{H}_\lambda(T) = \mathbf{P}_\lambda \mathbf{S}_Z(u) + \beta \int_0^T \mathrm{d}W(t)\, z(t)^\top. \tag{6}$$

The last term is a matrix-valued martingale with $\mathbb{E}[\int_0^T \mathrm{d}W(t)\, z(t)^\top] = 0$, hence $\mathbf{H}_\lambda(T) - \mathbf{P}_\lambda\mathbf{S}_Z(u)$ has zero mean.

Deterministic identity and a derivative-free margin. If x is absolutely continuous and $\beta = 0$, then $\mathrm{d}y_\lambda(t) = m_\lambda(t)\,\mathrm{d}t$ and therefore

$$\mathbf{H}_\lambda(T) = \int_0^T m_\lambda(t)\, z(t)^\top\,\mathrm{d}t = \mathbf{P}_\lambda\mathbf{S}_Z(u). \tag{7}$$

If moreover $\mathbf{S}_Z(u)$ is invertible, then the continuous-time Gramian admits the fully derivative-free representation

$$\mathbf{G}_\lambda(u) = \mathbf{H}_\lambda(T)\mathbf{S}_Z(u)^{-1}\mathbf{H}_\lambda(T)^*, \tag{8}$$

and

$$\sigma_{\min}\Big(\mathbf{G}_\lambda(u)\Big) = \sigma_{\min}\Big(\mathbf{H}_\lambda(T)\mathbf{S}_Z(u)^{-1/2}\Big)^2 \geq \sigma_{\min}(\mathbf{P}_\lambda)^2\,\sigma_{\min}\Big(\mathbf{S}_Z(u)\Big), \tag{9}$$

where $\mathbf{S}_Z(u)^{-1/2}$ denotes the unique symmetric square root of $\mathbf{S}_Z(u)^{-1}$.

Corollary 3.2 (Continuous Hautus test via cross-moments)**.** *Assume x is absolutely continuous, $\beta = 0$, and $\mathbf{S}_Z(u)$ is invertible. Then $(\mathbf{A},\mathbf{B})$ is controllable if and only if* $\operatorname{rank}(\mathbf{H}_\lambda(T)) = n$ *for all $\lambda \in \mathbb{C}$. Equivalently,*

$$(\mathbf{A},\mathbf{B})\ \textit{controllable} \quad\Longleftrightarrow\quad \inf_{\lambda\in\mathbb{C}} \sigma_{\min}\Big(\mathbf{H}_\lambda(T)\mathbf{S}_Z(u)^{-1/2}\Big) > 0.$$

Proof. See Appendix A.2. □

Estimating $\mathbf{P}_\lambda$. Assume that $\mathbf{S}_Z(u)$ is invertible and define

$$\widehat{\mathbf{P}}_\lambda(T) := \mathbf{H}_\lambda(T)\mathbf{S}_Z(u)^{-1}. \tag{10}$$

Then (6) implies the exact error identity

$$\widehat{\mathbf{P}}_\lambda(T) - \mathbf{P}_\lambda = \beta\left(\int_0^T \mathrm{d}W(t)\, z(t)^\top\right)\mathbf{S}_Z(u)^{-1}. \tag{11}$$

A basic $T^{-1/2}$ rate via Itô isometry. Introduce the normalized quantities $\bar{\mathbf{S}}_Z(T) := \frac{1}{T}\mathbf{S}_Z(u)$ and $\bar{\mathbf{H}}_\lambda(T) := \frac{1}{T}\mathbf{H}_\lambda(T)$ so that $\widehat{\mathbf{P}}_\lambda(T) = \bar{\mathbf{H}}_\lambda(T)\bar{\mathbf{S}}_Z(T)^{-1}$. The Itô isometry yields (componentwise) the bound

$$\mathbb{E}\left\|\frac{1}{T}\int_0^T \mathrm{d}W(t)\, z(t)^\top\right\|_F^2 = \frac{q}{T^2}\mathbb{E}\left[\int_0^T \|z(t)\|_2^2\,\mathrm{d}t\right]. \tag{12}$$

If $\mathbb{E}[\int_0^T \|z(t)\|_2^2\,\mathrm{d}t] = \mathcal{O}(T)$ and $\|\bar{\mathbf{S}}_Z(T)^{-1}\|_2 = \mathcal{O}_{\mathbb{P}}(1)$, then (11) and (12) imply

$$\|\widehat{\mathbf{P}}_\lambda(T) - \mathbf{P}_\lambda\|_2 = \mathcal{O}_{\mathbb{P}}(T^{-1/2}). \tag{13}$$

The $\mathcal{O}_{\mathbb{P}}(T^{-1/2})$ statement above can be strengthened to an explicit bound holding with probability $1-\delta$ and depending only on the (random) conditioning of $\bar{\mathbf{S}}_Z(T)$.

Proposition 3.3 (Cross-moment error bound)**.** *Assume that $\mathbf{S}_Z(u) \succ 0$. Then for every $\delta \in (0,1)$, with probability at least $1-\delta$,*

$$\|\widehat{\mathbf{P}}_\lambda(T) - \mathbf{P}_\lambda\|_2 \le \frac{\|\beta\|_2}{\sqrt{T\,\sigma_{\min}(\bar{\mathbf{S}}_Z(T))}}\left(\sqrt{q} + \sqrt{n+m} + \sqrt{2\log(1/\delta)}\right). \tag{14}$$

Moreover, this implies the uniform bound $\sup_{\lambda\in\mathbb{C}} \|\widehat{\mathbf{P}}_\lambda(T) - \mathbf{P}_\lambda\|_2$ since the right-hand side of (11) does not depend on λ.

Proof. See Appendix A.3. □

Finally, by Weyl's inequality,

$$\left|\sigma_{\min}\left(\widehat{\mathbf{P}}_\lambda(T)\right) - \sigma_{\min}(\mathbf{P}_\lambda)\right| \le \|\widehat{\mathbf{P}}_\lambda(T) - \mathbf{P}_\lambda\|_2,$$

which provides a simple statistical analogue of the deterministic Hautus margin. In particular, Proposition 3.3 yields a corresponding $(1-\delta)$ bound on the singular-value deviation.

A Fourier-domain approximation without derivatives. The cross-moment $\mathbf{H}_\lambda(T)$ in (5) can also be approximated in the frequency domain without forming $\dot{x}$. For each $\omega \in \mathbb{R}$, define the Fourier transform of the residual increment

$$\widehat{dy}_\lambda(\mathrm{i}\omega) := \int_0^T e^{-\mathrm{i}\omega t}\,\mathrm{d}y_\lambda(t) = \int_0^T e^{-\mathrm{i}\omega t}\,\mathrm{d}x(t) - \lambda\widehat{x}(\mathrm{i}\omega), \qquad \widehat{x}(\mathrm{i}\omega) := \int_0^T x(t)e^{-\mathrm{i}\omega t}\,\mathrm{d}t.$$

Since $t \mapsto e^{-\mathrm{i}\omega t}$ is of bounded variation, Itô integration by parts yields

$$\int_0^T e^{-\mathrm{i}\omega t}\,\mathrm{d}x(t) = x(T)e^{-\mathrm{i}\omega T} - x(0) + \mathrm{i}\omega\int_0^T x(t)e^{-\mathrm{i}\omega t}\,\mathrm{d}t,$$

hence

$$\widehat{dy}_\lambda(\mathrm{i}\omega) = x(T)e^{-\mathrm{i}\omega T} - x(0) + (\mathrm{i}\omega - \lambda)\widehat{x}(\mathrm{i}\omega). \tag{15}$$

Thus, $\widehat{dy}_\lambda(\mathrm{i}\omega)$ can be computed from an FFT of x plus the boundary terms $x(0), x(T)$. Define also $\widehat{z}(\mathrm{i}\omega) := \int_0^T z(t)e^{-\mathrm{i}\omega t}\,\mathrm{d}t$. If x is absolutely continuous so that $\mathrm{d}y_\lambda(t) = m_\lambda(t)\,\mathrm{d}t$, then Parseval gives

$$\mathbf{H}_\lambda(T) = \int_{\mathbb{R}} \widehat{dy}_\lambda(\mathrm{i}\omega)\widehat{z}(\mathrm{i}\omega)^*\,\frac{\mathrm{d}\omega}{2\pi}, \qquad \mathbf{S}_Z(u) = \int_{\mathbb{R}} \widehat{z}(\mathrm{i}\omega)\widehat{z}(\mathrm{i}\omega)^*\,\frac{\mathrm{d}\omega}{2\pi}.$$

In the Itô setting, the unwindowed energy $\int_{\mathbb{R}} \|\widehat{dy}_\lambda(\mathrm{i}\omega)\|_2^2\,\mathrm{d}\omega$ is not finite (it corresponds to the L^2-energy of a derivative that does not exist), so frequency-domain computations should be interpreted with an explicit cutoff/windowing when needed.

3.3. **An operator formulation and finitely many candidate λ.** The main inconvenience of Theorem 3.1 is that the margin condition must hold for all $\lambda \in \mathbb{C}$. To address this, we now develop an operator formulation that allows us to identify finitely many candidate λ where rank failure can occur. Let $x : [0,T] \to \mathbb{R}^n$ be absolutely continuous with $x, \dot{x} \in L^2(0,T;\mathbb{R}^n)$ and define operators

$$\mathcal{X}, \dot{\mathcal{X}} : L^2(0,T) \to \mathbb{C}^n, \qquad \mathcal{X}(\varphi) := \int_0^T x(t)\varphi(t)\,\mathrm{d}t, \quad \dot{\mathcal{X}}(\varphi) := \int_0^T \dot{x}(t)\varphi(t)\,\mathrm{d}t.$$

For $\lambda \in \mathbb{C}$, define the pencil of operators

$$\mathcal{P}(\lambda) := \dot{\mathcal{X}} - \lambda \mathcal{X}.$$

Since the codomain is finite-dimensional, $\operatorname{rank}(\mathcal{P}(\lambda)) := \dim(\operatorname{range}(\mathcal{P}(\lambda))) \le n$, and *full rank* means surjectivity onto $\mathbb{C}^n$. For $\varphi \in L^2(0,T)$ and $w \in \mathbb{C}^n$,

$$\langle \mathcal{X}(\varphi), w\rangle_{\mathbb{C}^n} = \Big(\int_0^T x(t)\varphi(t)\,\mathrm{d}t\Big)^* w = \int_0^T \overline{\varphi(t)}\, x(t)^* w\,\mathrm{d}t = \langle \varphi,\, x(\cdot)^* w\rangle_{L^2(0,T)}.$$

Repeating the same process for $\dot{\mathcal{X}}$ yields

$$(\mathcal{X}^* w)(t) = x(t)^* w, \qquad (\dot{\mathcal{X}}^* w)(t) = \dot{x}(t)^* w \qquad \text{in } L^2(0,T),$$

Therefore, for $w \in \mathbb{C}^n$,

$$\mathcal{P}(\lambda)\mathcal{P}(\lambda)^* w = \mathcal{P}(\lambda)\big(\dot{\mathcal{X}}^* w - \overline{\lambda}\mathcal{X}^* w\big) = \int_0^T m_\lambda(t)\, m_\lambda(t)^* w\,\mathrm{d}t = \mathbf{G}_\lambda(u)\, w.$$

Hence,

$$\mathcal{P}(\lambda)\mathcal{P}(\lambda)^* = \mathbf{G}_\lambda(u) \qquad \text{as operators } \mathbb{C}^n \to \mathbb{C}^n. \tag{16}$$

Since $\mathcal{P}(\lambda) : L^2(0,T) \to \mathbb{C}^n$ has finite-dimensional codomain, it is surjective if and only if $\mathcal{P}(\lambda)\mathcal{P}(\lambda)^*$ is invertible on $\mathbb{C}^n$. By (16), for every $\lambda \in \mathbb{C}$,

$$\operatorname{rank}(\mathcal{P}(\lambda)) = n \quad \Leftrightarrow \quad \mathbf{G}_\lambda(u) \text{ is invertible.} \tag{17}$$

The next result shows that, under a mild nondegeneracy assumption, rank failure can only occur at finitely many "candidate" values of λ.

Theorem 3.4 (Finite candidate set for $\lambda \in \mathbb{C}$)**.** *Assume* $\operatorname{rank}(\mathcal{X}) = n$*, equivalently*

$$\mathcal{X}\mathcal{X}^* = \int_0^T x(t)x(t)^*\,\mathrm{d}t \in \mathbb{C}^{n\times n} \quad \textit{is invertible.}$$

This is a data-richness condition: it requires, in particular, that the trajectory does not remain in a strict subspace of $\mathbb{R}^n$ *on* $[0,T]$*. Define*

$$\mathbf{K} := (\mathcal{X}\mathcal{X}^*)^{-1}\mathcal{X}\dot{\mathcal{X}}^* \in \mathbb{C}^{n\times n}.$$

Then for every $\lambda \in \mathbb{C}$*,*

$$\operatorname{rank}(\mathcal{P}(\lambda)) < n \quad \Longrightarrow \quad \lambda \in \sigma(\mathbf{K}).$$

In particular, the set of λ *for which* $\operatorname{rank}(\mathcal{P}(\lambda)) < n$ *is contained in* $\sigma(\mathbf{K})$*, which has at most* n *elements. Moreover, in terms of time-domain moments,*

$$\mathbf{K} = \Big(\int_0^T x(t)x(t)^*\,\mathrm{d}t\Big)^{-1}\Big(\int_0^T x(t)\dot{x}(t)^*\,\mathrm{d}t\Big).$$

Proof. See Appendix A.4. □

Corollary 3.5 (Finite checking). *Under the assumptions of Theorem 3.4, if*

$$\operatorname{rank}(\mathcal{P}(\lambda)) = n \qquad \text{for all } \lambda \in \sigma(\mathbf{K}),$$

then $\operatorname{rank}(\mathcal{P}(\lambda)) = n$ *for all* $\lambda \in \mathbb{C}$.

Proof. See Appendix A.5. □

Lemma 3.6 (A quantitative lower bound for $\sigma_{\min}(\mathbf{G}_\lambda(u))$ via $\mathbf{K}$). *Assume* $\operatorname{rank}(\mathcal{X}) = n$ *and let* $\mathbf{K}$ *be as in Theorem 3.4. Then for every* $\lambda \in \mathbb{C}$,

$$\sigma_{\min}\Big(\mathbf{G}_\lambda(u)\Big) \geq \frac{\sigma_{\min}(\mathbf{K} - \overline{\lambda}\,\mathbf{I})^2}{\|(\mathcal{X}\mathcal{X}^*)^{-1}\mathcal{X}\|^2}.$$

In particular, if $\lambda \notin \sigma(\mathbf{K})$, *then* $\mathbf{G}_\lambda(u)$ *is invertible and* $\sigma_{\min}(\mathbf{G}_\lambda(u)) > 0$.

Proof. See Appendix A.6. □

Consequently, for rank certification it is enough to check the finitely many candidates $\sigma(\mathbf{K})$.

Remark 3.7 (Frequency-domain calculation). *The matrix* $\mathbf{K}$ *in Theorem 3.4 can be computed from the Fourier transforms of* x *and* $\dot{x}$ *as*

$$\mathbf{K} = \Big(\int_{\mathbb{R}} \widehat{x}(\mathrm{i}\omega)\widehat{x}(\mathrm{i}\omega)^* \frac{\mathrm{d}\omega}{2\pi}\Big)^{-1}\Big(\int_{\mathbb{R}} \widehat{x}(\mathrm{i}\omega)\widehat{\dot{x}}(\mathrm{i}\omega)^* \frac{\mathrm{d}\omega}{2\pi}\Big),$$

where we know that $\widehat{\dot{x}}(\mathrm{i}\omega) = x(T)e^{-\mathrm{i}\omega T} - x(0) + \mathrm{i}\omega\widehat{x}(\mathrm{i}\omega)$.

3.4. **Best conditioning of control inputs.** The data-driven Hautus margins in Corollary 3.2 are controlled (up to the model-dependent factor $\sigma_{\min}(\mathbf{P}_\lambda)$) by the smallest singular value of the stacked Gramian $\mathbf{S}_Z(u)$. Since $\mathbf{S}_Z(u)$ depends on the unknown response $x(\cdot)$, a natural model-agnostic surrogate is to ensure that the *input* Gramian is well conditioned, so that the input directions are persistently excited and the inversion of $\mathbf{S}_Z(u)$ in (8) is numerically stable. Under an L^2 energy budget, the best possible conditioning corresponds to spreading the energy isotropically across the m input channels.

Proposition 3.8 (Best conditioning of the input Gramian under $\|u\|_{L^2} \leq 1$). *Define the input Gramian*

$$\mathbf{S}_U(u) := \int_0^T u(t)u(t)^\top \,\mathrm{d}t \in \mathbb{R}^{m\times m}.$$

If $\|u\|^2_{L^2(0,T)} \leq 1$, *then*

$$\lambda_{\min}(\mathbf{S}_U(u)) \leq \frac{1}{m}.$$

Moreover, there exist u *with* $\|u\|_{L^2(0,T)} \leq 1$ *such that* $\mathbf{S}_U(u) = \frac{1}{m}\mathbf{I}_m$. *In particular, the upper bound is tight.*

Proof. See Appendix A.7. □

Remark 3.9. *The matrix* $\mathbf{S}_U(u)$ *is a principal submatrix of* $\mathbf{S}_Z(u)$, *hence*

$$\sigma_{\min}(\mathbf{S}_Z(u)) \leq \sigma_{\min}(\mathbf{S}_U(u)).$$

Thus, even though $\sigma_{\min}(\mathbf{S}_Z(u))$ *depends on the state-response, and therefore on* $(\mathbf{A}, \mathbf{B})$ *and the initial condition, choosing inputs with well-conditioned* $\mathbf{S}_U(u)$ *is a natural baseline when seeking a large* $\sigma_{\min}(\mathbf{S}_Z(u))$ *without model knowledge.*

3.5. **Best conditioning under an H^1 budget.** In applications one may also constrain input *smoothness*, for instance by an H^1 budget

$$\|u\|^2_{H^1(0,T)} := \int_0^T \left(\|u(t)\|_2^2 + \|\dot{u}(t)\|_2^2\right) \mathrm{d}t \le 1.$$

This penalizes high-frequency excitation and therefore reduces the best achievable isotropic conditioning compared to the L^2-only case.

Proposition 3.10 (H^1-budget isotropic input)**.** *Let $u \in H^1(0,T;\mathbb{R}^m)$ satisfy $\|u\|_{H^1(0,T)} \le 1$, and define $\mathbf{S}_U(u) := \int_0^T u(t)u(t)^\top \mathrm{d}t$. Then*

$$\lambda_{\min}(\mathbf{S}_U(u)) \le \frac{1}{\sum_{k=0}^{m-1}\left(1 + \left(\frac{k\pi}{T}\right)^2\right)} = \frac{1}{m + \frac{\pi^2}{T^2}\cdot\frac{(m-1)m(2m-1)}{6}}.$$

Moreover, the bound is tight: if $\{\psi_k\}_{k\ge 0}$ are the Neumann eigenfunctions on $[0,T]$ given by

$$\psi_0(t) := \frac{1}{\sqrt{T}}, \qquad \psi_k(t) := \sqrt{\frac{2}{T}}\cos\left(\frac{k\pi t}{T}\right) \ (k \ge 1),$$

and $Q \in \mathbb{R}^{m\times m}$ is orthogonal, then with

$$\alpha := \left(\sum_{k=0}^{m-1}\left(1 + (\tfrac{k\pi}{T})^2\right)\right)^{-1}, \qquad u(t) := \sqrt{\alpha}\, Q \begin{bmatrix} \psi_0(t) \\ \vdots \\ \psi_{m-1}(t) \end{bmatrix},$$

one has $\|u\|^2_{H^1(0,T)} = 1$ and $\mathbf{S}_U(u) = \alpha\, \mathbf{I}_m$.

Proof. See Appendix A.8. □

Remark 3.11. *As $T \to \infty$ the derivative penalty vanishes and $\alpha \to 1/m$, recovering the L^2-budget optimum in Proposition 3.8. For short horizons (or large m), the optimal H^1-budget design suppresses high-frequency components and yields a smaller isotropic eigenvalue α.*

4. Numerical Experiments

We validate the theoretical results with numerical experiments implemented in PyTorch. We simulate controlled linear SDEs of the form

$$\mathrm{d}x(t) = (\mathbf{A}x(t) + \mathbf{B}u(t))\,\mathrm{d}t + \beta\,\mathrm{d}W(t),$$

using Euler–Maruyama time stepping.

4.1. **Validation of the Data-Driven Hautus Test.** Our first experiment validates the data-driven Hautus test by comparing the estimated matrix $\widehat{\mathbf{P}}_\lambda$ with the true Hautus matrix $\mathbf{P}_\lambda = [\mathbf{A} - \lambda\mathbf{I} \mid \mathbf{B}]$. We simulate a system with $n = 6$ states, $m = 3$ inputs, and $q = 2$ noise dimensions over a horizon $T = 100$ with time step $\mathrm{d}t = 0.05$. The drift matrix $\mathbf{A}$ is constructed to be stable with eigenvalues having real parts bounded by -0.1.

For each $\lambda \in \mathbb{C}$, we compute both time-domain and FFT-based estimates via the cross-moment formulation (10).

Figure 1 shows the element-wise comparison between the true and estimated matrices for a representative $\lambda = 0.3 + 1.3\mathrm{i}$. Both methods yield accurate estimates, with estimation errors $\|\widehat{\mathbf{P}}_\lambda - \mathbf{P}_\lambda\|_2$ on the order of 10^{-2}. To assess variability, we run 50 independent trajectories and examine the distribution of errors across the eigenvalues of $\mathbf{A}$ and additional random test points. Figure 2 (left) summarizes the signed error $\sigma_{\min}(\mathbf{P}_\lambda) - \sigma_{\min}(\widehat{\mathbf{P}}_\lambda)$, showing near-zero bias and comparable variance for time-domain and FFT estimators.

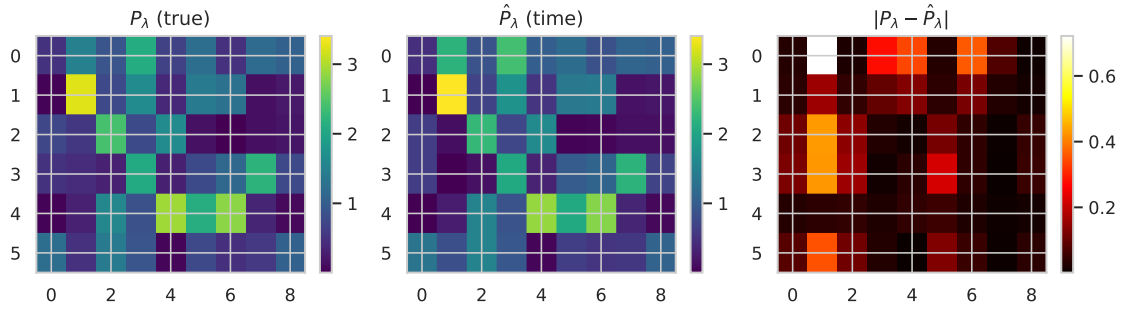

FIGURE 1. Element-wise comparison of the true Hautus matrix $\mathbf{P}_\lambda$ (left) and its time-domain estimate $\widehat{\mathbf{P}}_\lambda$ (center), with absolute difference (right). The small difference magnitudes confirm the accuracy of the cross-moment estimator.

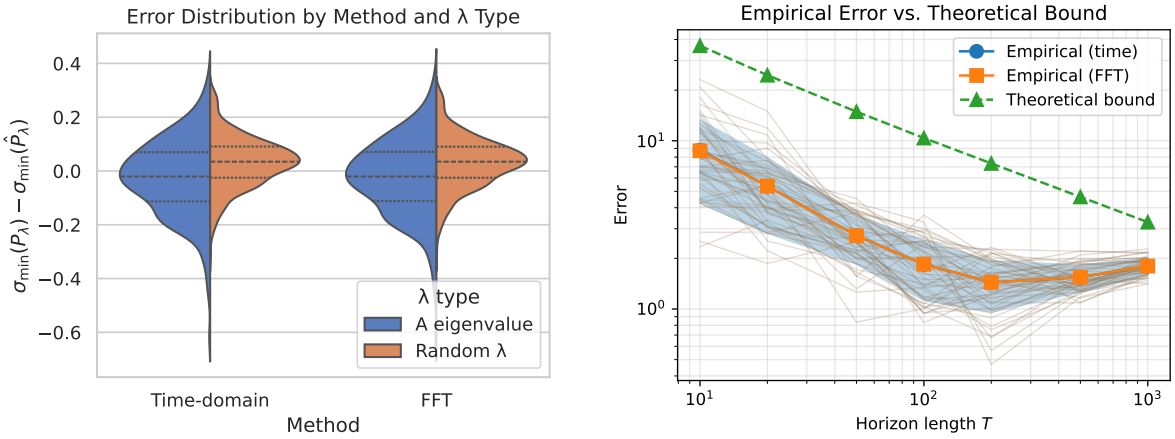

(A) Error distribution across 50 trajectories (eigenvalues of $\mathbf{A}$ and random test points).

(B) Mean error versus horizon T (log-log) with ± 1 std shading and the theoretical bound.

FIGURE 2. Summary of estimation accuracy: variability across trials (left) and $T^{-1/2}$ convergence (right).

4.2. **Error Convergence Rate.** Proposition 3.3 predicts that the estimation error $\|\widehat{\mathbf{P}}_\lambda - \mathbf{P}_\lambda\|_2$ decays as $\mathcal{O}(T^{-1/2})$. We validate this rate by simulating systems with $n = 5$, $m = 3$, $q = 2$ for horizon lengths $T \in \{10, 20, 50, 100, 200, 500, 1000\}$. For each T, we run 50 Monte Carlo trials with independent noise realizations and random test eigenvalues λ.

Figure 2 (right) presents the results on a log-log scale. The empirical mean errors for both time-domain and FFT methods closely follow the $T^{-1/2}$ rate. The shaded region indicates ± 1 standard deviation across trials. We also overlay the theoretical bound from Proposition 3.3 (computed with $\delta = 0.05$), which provides a valid upper envelope for the empirical errors. A linear regression on the log-transformed data yields an estimated slope of approximately -0.5, confirming the theoretical rate.

4.3. **Finite Candidate Eigenvalue Check.** A key practical advantage of the cross-moment formulation is that controllability can be verified by testing only a finite set of candidate eigenvalues rather than all $\lambda \in \mathbb{C}$. Specifically, the operator formulation (Section 3.3) shows that

$\omega_{\max}$	$\sigma_{\min}(\widehat{\mathbf{P}}_\lambda)$	$\|\widehat{\mathbf{P}}_\lambda - \mathbf{P}_\lambda\|_2$
10	0.412	0.089
20	0.428	0.051
50	0.435	0.027
100	0.438	0.018
200	0.439	0.015
∞ (all)	0.439	0.014

TABLE 1. Effect of frequency cutoff on FFT method accuracy.

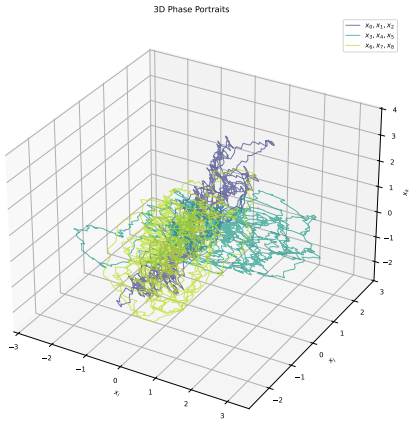

FIGURE 3. Three-dimensional phase portraits for (x_0, x_1, x_2), (x_3, x_4, x_5), and (x_6, x_7, x_8).

the candidates are the eigenvalues of the matrix $\mathbf{K} = \mathbf{S}_X^{-1}\mathbf{M}_X$, where $\mathbf{S}_X = \int_0^T x(t)x(t)^\top \, \mathrm{d}t$ and $\mathbf{M}_X = \int_0^T x(t) \, \mathrm{d}x(t)^\top$.

We simulate a controllable system with $n = 6$, $m = 3$, $q = 2$ over $T = 100$. The candidate eigenvalues $\sigma(\mathbf{K})$ are computed from the trajectory data and compared with the true eigenvalues $\sigma(\mathbf{A})$. For each candidate λ_i, we compute the estimated minimum singular value $\sigma_{\min}(\widehat{\mathbf{P}}_{\lambda_i})$ and compare with the true value $\sigma_{\min}(\mathbf{P}_{\lambda_i})$.

The results show excellent agreement between estimated and true singular values across all candidates. The candidates $\sigma(\mathbf{K})$ cluster near the true eigenvalues $\sigma(\mathbf{A})$ in the complex plane, validating the theoretical prediction that the data-driven eigenvalue estimates converge to the true system eigenvalues. Since $\sigma_{\min}(\widehat{\mathbf{P}}_\lambda) > 0$ for all candidates, the system is correctly identified as controllable.

4.4. **Comparison of Time-Domain and FFT Methods.** We compare the time-domain and FFT-based computation methods for the cross-moments. The time-domain method computes $\mathbf{H}_\lambda(T)$ via direct numerical integration, while the FFT method uses the Parseval identity with frequency-domain representations (15).

For a system with $n = 8$, $m = 4$, $q = 2$ and $T = 100$ with fine time step $\mathrm{d}t = 0.02$ (yielding 5001 time points), we test both methods across various λ values. Both methods achieve comparable accuracy, with estimation errors typically differing by less than 10%.

The FFT method requires a frequency cutoff $\omega_{\max}$ to truncate the integral. Table 1 shows the effect of $\omega_{\max}$ on the estimation error for $\lambda = 0.3 + 0.8\mathrm{i}$. As expected, larger cutoffs improve accuracy, with diminishing returns beyond $\omega_{\max} \approx 100$. For compactness, we place Table 1 next to a representative 3D phase portrait (Figure 3).

In terms of computational efficiency, the FFT method offers modest speedups for long trajectories due to the $\mathcal{O}(N \log N)$ complexity of the FFT versus $\mathcal{O}(N)$ for direct integration, though both are fast in practice.

4.5. **Trajectory Visualization.** To provide intuition for the controlled stochastic dynamics, Figure 3 shows representative phase portraits for a 9-dimensional system with $m = 4$ inputs and $q = 2$ noise dimensions, simulated over $T = 50$ with a slowly decaying drift ($\mathbf{A}$ has eigenvalues with real parts near -0.05).

The phase portraits demonstrate that the stochastic input provides sufficient excitation to explore the state space, ensuring that the signal Gramian $\mathbf{S}_Z(u)$ is well-conditioned. This persistent excitation is crucial for accurate estimation of the Hautus matrix and reliable controllability certification.

References

[1] M.K. Camlibel et al. "The Shortest Experiment for Linear System Identification". In: *Systems & Control Letters* 197 (Mar. 2025), p. 106045. ISSN: 01676911. DOI: 10.1016/j.sysconle.2025.106045. URL: https://linkinghub.elsevier.com/retrieve/pii/S0167691125000271 (visited on 01/20/2026).

[2] Chi-Tsong Chen, ed. *Linear System Theory and Design*. 3rd ed. The Oxford Series in Electrical and Computer Engineering. New York: Oxford University Press, 1999. 334 pp. ISBN: 978-0-19-511777-6 978-1-61344-115-2 978-0-19-511778-3.

[3] Dennis Gramlich et al. *Fast Identification and Stabilization of Unknown Linear Systems*. arXiv.org. Aug. 22, 2022. URL: https://arxiv.org/abs/2208.10392v3 (visited on 12/11/2025).

[4] Andrea Iannelli et al. "Design of Input for Data-Driven Simulation with Hankel and Page Matrices". In: *2021 60th IEEE Conference on Decision and Control (CDC)*. 2021 60th IEEE Conference on Decision and Control (CDC). Dec. 2021, pp. 139–145. DOI: 10.1109/CDC45484.2021.9683709. URL: https://ieeexplore.ieee.org/document/9683709 (visited on 12/15/2025).

[5] R. E. Kalman. "Mathematical Description of Linear Dynamical Systems". In: *Journal of the Society for Industrial and Applied Mathematics Series A Control* 1.2 (Jan. 1963), pp. 152–192. ISSN: 0887-4603. DOI: 10.1137/0301010. URL: http://epubs.siam.org/doi/10.1137/0301010 (visited on 12/08/2025).

[6] Vikas Kumar Mishra et al. "Data-Driven Tests for Controllability". In: *IEEE Control Systems Letters* 5.2 (Apr. 2021), pp. 517–522. ISSN: 2475-1456. DOI: 10.1109/LCSYS.2020.3003770. URL: https://ieeexplore.ieee.org/document/9121339/ (visited on 12/11/2025).

[7] P. Rapisarda et al. "A "Fundamental Lemma" for Continuous-Time Systems, with Applications to Data-Driven Simulation". In: *Systems & Control Letters* 179 (Sept. 2023), p. 105603. ISSN: 01676911. DOI: 10.1016/j.sysconle.2023.105603. URL: https://linkinghub.elsevier.com/retrieve/pii/S0167691123001500 (visited on 01/20/2026).

[8] P. Rapisarda et al. "A Persistency of Excitation Condition for Continuous-Time Systems". In: *IEEE Control Systems Letters* 7 (2023), pp. 589–594. ISSN: 2475-1456. DOI: 10.1109/LCSYS.2022.3205550. URL: https://ieeexplore.ieee.org/document/9882335/ (visited on 01/20/2026).

[9] Amir Shakouri et al. "A New Perspective on Willems' Fundamental Lemma: Universality of Persistently Exciting Inputs". In: *IEEE Control Systems Letters* 9 (2025), pp. 583–588. ISSN: 2475-1456. DOI: 10.1109/LCSYS.2025.3576276. arXiv: 2503.12489 [math]. URL: http://arxiv.org/abs/2503.12489 (visited on 12/08/2025).

[10] Harry L. Trentelman et al. *Control Theory for Linear Systems*. Springer, 2001. ISBN: 978-1-85233-316-4. URL: https://research.utwente.nl/en/publications/control-theory-for-linear-systems/ (visited on 12/17/2025).

[11] Henk J. Van Waarde. "Beyond Persistent Excitation: Online Experiment Design for Data-Driven Modeling and Control". In: *IEEE Control Systems Letters* 6 (2022), pp. 319–324. ISSN: 2475-1456. DOI: 10.1109/LCSYS.2021.3073860. URL: https://ieeexplore.ieee.org/document/9406124/ (visited on 01/20/2026).

[12] Henk J. van Waarde et al. "Data Informativity: A New Perspective on Data-Driven Analysis and Control". In: *IEEE Transactions on Automatic Control* 65.11 (Nov. 2020), pp. 4753–4768. ISSN: 1558-2523. DOI: 10.1109/TAC.2020.2966717. URL: https://ieeexplore.ieee.org/document/8960476/ (visited on 12/11/2025).

[13] Roman Vershynin. "An Introduction with Applications in Data Science". In: ().

[14] Henk J. van Waarde et al. *Willems' Fundamental Lemma for State-space Systems and Its Extension to Multiple Datasets*. May 7, 2020. DOI: 10.48550/arXiv.2002.01023. arXiv: 2002.01023 [math]. URL: http://arxiv.org/abs/2002.01023 (visited on 12/08/2025). Pre-published.

[15] Jan C. Willems et al. "A Note on Persistency of Excitation". In: *Systems & Control Letters* 54.4 (Apr. 2005), pp. 325–329. ISSN: 01676911. DOI: 10.1016/j.sysconle.2004.09.003. URL: https://linkinghub.elsevier.com/retrieve/pii/S0167691104001434 (visited on 12/08/2025).

Appendix A. Proofs

A.1. Proof of the continuous-time Hautus test.

Proof. If $(\mathbf{A}, \mathbf{B})$ is not controllable, then by the (continuous-time) Hautus test there exist $\lambda \in \mathbb{C}$ and $v \neq 0$ such that $v^*\mathbf{P}_\lambda = 0$. Using (2), this gives $v^*\mathbf{G}_\lambda(u)v = v^*\mathbf{P}_\lambda \mathbf{S}_Z(u)\mathbf{P}_\lambda^* v = 0$, hence $\sigma_{\min}(\mathbf{G}_\lambda(u)) = 0$.

Conversely, assume $(\mathbf{A}, \mathbf{B})$ is controllable and $\mathbf{S}_Z(u)$ is invertible. Then $\mathbf{P}_\lambda$ has full row rank for every $\lambda \in \mathbb{C}$, so (2) implies $\mathbf{G}_\lambda(u) \succ 0$ for every λ. Moreover, since $\mathbf{S}_Z(u) \succ 0$, its state block $\mathbf{S}_X := \int_0^T x(t)x(t)^\top \, \mathrm{d}t$ satisfies $\mathbf{S}_X \succ 0$. Set $\mathbf{S}_{\dot{X}} := \int_0^T \dot{x}(t)\dot{x}(t)^\top \, \mathrm{d}t$. For any unit $v \in \mathbb{C}^n$,

$$v^*\mathbf{G}_\lambda(u)v = \left\| \dot{x}(\cdot)^* v - \overline{\lambda}\, x(\cdot)^* v \right\|_{L^2(0,T)}^2 \geq \left(|\lambda| \|x(\cdot)^* v\|_{L^2(0,T)} - \|\dot{x}(\cdot)^* v\|_{L^2(0,T)} \right)^2.$$

Using $\|x(\cdot)^* v\|_{L^2(0,T)}^2 = v^*\mathbf{S}_X v \geq \lambda_{\min}(\mathbf{S}_X)$ and $\|\dot{x}(\cdot)^* v\|_{L^2(0,T)}^2 = v^*\mathbf{S}_{\dot{X}} v \leq \lambda_{\max}(\mathbf{S}_{\dot{X}})$ yields the uniform lower bound

$$\sigma_{\min}(\mathbf{G}_\lambda(u)) \geq \left(|\lambda| \sqrt{\lambda_{\min}(\mathbf{S}_X)} - \sqrt{\lambda_{\max}(\mathbf{S}_{\dot{X}})} \right)^2,$$

hence $\sigma_{\min}(\mathbf{G}_\lambda(u)) \to \infty$ as $|\lambda| \to \infty$. Since $\lambda \mapsto \sigma_{\min}(\mathbf{G}_\lambda(u))$ is continuous and strictly positive, it attains a positive minimum on a large enough closed ball in $\mathbb{C}$, and the coercivity above controls the complement. Therefore $\inf_{\lambda \in \mathbb{C}} \sigma_{\min}(\mathbf{G}_\lambda(u)) > 0$. □

A.2. Proof of the cross-moment Hautus test.

Proof. Under the stated assumptions, (7) holds, hence $\mathbf{H}_\lambda(T)\mathbf{S}_Z(u)^{-1/2} = \mathbf{P}_\lambda \mathbf{S}_Z(u)^{1/2}$ and $\mathbf{G}_\lambda(u) = \left(\mathbf{H}_\lambda(T)\mathbf{S}_Z(u)^{-1/2}\right)\left(\mathbf{H}_\lambda(T)\mathbf{S}_Z(u)^{-1/2}\right)^*$. Therefore $\operatorname{rank}(\mathbf{H}_\lambda(T)) = n$ for all λ if and only if $\mathbf{G}_\lambda(u) \succ 0$ for all λ. The claim then follows from Theorem 3.1. □

A.3. **Proof of the cross-moment error bound.**

Proof. Let $\mathbf{M}(T) := \int_0^T \mathrm{d}W(t)\, z(t)^\top \in \mathbb{R}^{q\times(n+m)}$. Conditional on the path $\{z(t)\}_{t\in[0,T]}$, $\mathbf{M}(T)$ is a centered Gaussian matrix whose rows are independent and satisfy

$$\mathbb{E}\Big[\mathbf{M}(T)_{i,:}^\top \mathbf{M}(T)_{i,:} \mid z\Big] = \int_0^T z(t)z(t)^\top \,\mathrm{d}t = \mathbf{S}_Z(u), \qquad i = 1,\dots,q.$$

Therefore, conditional on z, we have the distributional identity $\mathbf{M}(T) \overset{d}{=} \mathbf{G}\mathbf{S}_Z(u)^{1/2}$ where $\mathbf{G} \in \mathbb{R}^{q\times(n+m)}$ has i.i.d. $\mathcal{N}(0,1)$ entries. Using (11),

$$\widehat{\mathbf{P}}_\lambda(T) - \mathbf{P}_\lambda \overset{d}{=} \beta\, \mathbf{G}\mathbf{S}_Z(u)^{-1/2},$$

conditional on z, hence

$$\|\widehat{\mathbf{P}}_\lambda(T) - \mathbf{P}_\lambda\|_2 \le \frac{\|\beta\|_2}{\sqrt{\sigma_{\min}(\mathbf{S}_Z(u))}}\, \|\mathbf{G}\|_2.$$

The standard Gaussian matrix bound $\mathbb{P}\Big(\|\mathbf{G}\|_2 \ge \sqrt{q} + \sqrt{n+m} + t\Big) \le e^{-t^2/2}$ (valid for all $t \ge 0$; see, e.g., [13]) yields (14) by choosing $t = \sqrt{2\log(1/\delta)}$ and using $\sigma_{\min}(\mathbf{S}_Z(u)) = T\sigma_{\min}(\bar{\mathbf{S}}_Z(T))$. □

A.4. **Proof of the finite candidate set result.**

Proof. Fix $\lambda \in \mathbb{C}$ and assume $\operatorname{rank}(\mathcal{P}(\lambda)) < n$. Since the codomain is $\mathbb{C}^n$, the left nullspace is nontrivial, so there exists $0 \ne w \in \mathbb{C}^n$ with $\mathcal{P}(\lambda)^* w = 0$, i.e. $\dot{\mathcal{X}}^* w = \overline{\lambda}\mathcal{X}^* w$. Left-multiply by $(\mathcal{X}\mathcal{X}^*)^{-1}\mathcal{X}$ to obtain

$$\mathbf{K}w = (\mathcal{X}\mathcal{X}^*)^{-1}\mathcal{X}\dot{\mathcal{X}}^* w = \overline{\lambda}\,(\mathcal{X}\mathcal{X}^*)^{-1}\mathcal{X}\mathcal{X}^* w = \overline{\lambda}\, w,$$

so $\overline{\lambda} \in \sigma(\mathbf{K})$. Since x is real-valued, the moments defining $\mathbf{K}$ are real and hence $\sigma(\mathbf{K})$ is closed under complex conjugation, which yields $\lambda \in \sigma(\mathbf{K})$. □

A.5. **Proof of the finite checking corollary.**

Proof. If there existed $\lambda_0 \in \mathbb{C}$ with $\operatorname{rank}(\mathcal{P}(\lambda_0)) < n$, then Theorem 3.4 would imply $\lambda_0 \in \sigma(\mathbf{K})$, contradicting the hypothesis. □

A.6. **Proof of the quantitative margin bound.**

Proof. Fix $w \in \mathbb{C}^n$. Since $w^*(\dot{\mathcal{X}} - \lambda\mathcal{X})$ is a bounded linear functional on $L^2(0,T)$, we have

$$\big\|w^*(\dot{\mathcal{X}} - \lambda\mathcal{X})\big\| = \big\|(\dot{\mathcal{X}}^* - \overline{\lambda}\,\mathcal{X}^*)w\big\|_{L^2(0,T)}.$$

Moreover,

$$(\mathbf{K} - \overline{\lambda}\,\mathbf{I})w = (\mathcal{X}\mathcal{X}^*)^{-1}\mathcal{X}(\dot{\mathcal{X}}^* - \overline{\lambda}\,\mathcal{X}^*)w,$$

hence

$$\|(\mathbf{K} - \overline{\lambda}\,\mathbf{I})w\| \le \|(\mathcal{X}\mathcal{X}^*)^{-1}\mathcal{X}\|\, \big\|(\dot{\mathcal{X}}^* - \overline{\lambda}\,\mathcal{X}^*)w\big\|_{L^2(0,T)}.$$

Using (16), $\|(\dot{\mathcal{X}}^* - \overline{\lambda}\,\mathcal{X}^*)w\|_{L^2(0,T)}^2 = w^*\mathbf{G}_\lambda(u)w$, so

$$w^*\mathbf{G}_\lambda(u)w \ge \frac{\|(\mathbf{K} - \overline{\lambda}\,\mathbf{I})w\|^2}{\|(\mathcal{X}\mathcal{X}^*)^{-1}\mathcal{X}\|^2}.$$

Taking the minimum over $\|w\|_2 = 1$ yields the claimed bound. The final claim follows since $\sigma_{\min}(\mathbf{K} - \overline{\lambda}\,\mathbf{I}) > 0$ whenever $\lambda \notin \sigma(\mathbf{K})$. □

A.7. **Proof of the L^2-budget isotropic design.**

Proof. Since $\mathbf{S}_U(u) \succeq 0$, we have $\lambda_{\min}(\mathbf{S}_U(u)) \le \frac{1}{m}\operatorname{tr}(\mathbf{S}_U(u))$. Moreover,

$$\operatorname{tr}(\mathbf{S}_U(u)) = \int_0^T \operatorname{tr}\big(u(t)u(t)^\top\big)\,\mathrm{d}t = \int_0^T \|u(t)\|_2^2\,\mathrm{d}t = \|u\|_{L^2(0,T)}^2 \le 1,$$

which gives the upper bound. For achievability, pick an orthonormal set $\{\varphi_i\}_{i=1}^m \subset L^2(0,T)$ and define $u(t) := \frac{1}{\sqrt{m}}[\varphi_1(t)\ \cdots\ \varphi_m(t)]^\top$; then $\mathbf{S}_U(u) = \frac{1}{m}\mathbf{I}_m$. □

A.8. **Proof of the H^1-budget isotropic design.**

Proof. Expand u in the orthonormal Neumann basis $\{\psi_k\}_{k\ge0}$ as $u(t) = \sum_{k\ge0}\psi_k(t)a_k$ with coefficients $a_k \in \mathbb{R}^m$, so that

$$\mathbf{S}_U(u) = \sum_{k\ge0} a_k a_k^\top, \qquad \|u\|_{H^1(0,T)}^2 = \sum_{k\ge0}\left(1 + \left(\tfrac{k\pi}{T}\right)^2\right)\|a_k\|_2^2.$$

Let $W := \operatorname{diag}(w_0, w_1, \dots)$ with $w_k := 1 + (\frac{k\pi}{T})^2$, and define $A := [a_0\ a_1\ \cdots]$, so that $\mathbf{S}_U(u) = AA^\top$ and $\|u\|_{H^1(0,T)}^2 = \operatorname{tr}(AWA^\top)$. Write $A = \mathbf{S}_U(u)^{1/2}R$ where R has orthonormal rows ($RR^\top = \mathbf{I}_m$), and set $\Pi := R^\top R$, a rank-m orthogonal projector. Then

$$\begin{aligned}
\|u\|_{H^1(0,T)}^2 &= \operatorname{tr}\big(\mathbf{S}_U(u)^{1/2}RWR^\top\mathbf{S}_U(u)^{1/2}\big)\\
&= \operatorname{tr}\big(\mathbf{S}_U(u)\,RWR^\top\big)\\
&\ge \lambda_{\min}(\mathbf{S}_U(u))\ \operatorname{tr}(RWR^\top)\\
&= \lambda_{\min}(\mathbf{S}_U(u))\ \operatorname{tr}(W\Pi).
\end{aligned}$$

Since W is diagonal with nondecreasing entries, the minimum of $\operatorname{tr}(W\Pi)$ over rank-m projectors Π equals $\sum_{k=0}^{m-1} w_k$, attained by projecting onto $\operatorname{span}\{\psi_0, \dots, \psi_{m-1}\}$. Using $\|u\|_{H^1(0,T)}^2 \le 1$ gives the stated upper bound on $\lambda_{\min}(\mathbf{S}_U(u))$. The construction with the first m Neumann modes and orthogonal Q yields $\mathbf{S}_U(u) = \alpha\mathbf{I}_m$ and saturates $\|u\|_{H^1(0,T)}^2 = 1$. □